ADVANCING EARTH AND SPACE SCIENCE

Global Biogeochemical Cycles

RESEARCH ARTICLE

10.1029/2021GB007038

Contrasting Responses of Soil Inorganic Carbon to Afforestation in Acidic Versus Alkaline Soils

Songbai Hong[1] and **Anping Chen**[2]

[1]Sino-French Institute for Earth System Science, College of Urban and Environmental Sciences, Peking University, Beijing, China, [2]Department of Biology and Graduate Degree Program in Ecology, Colorado State University, Fort Collins, CO, USA

Key Points:

- We conducted an extensive field survey investigating the impact of afforestation on soil inorganic carbon (SIC)
- Soil pH was a key variable mediating SIC responses to afforestation, which enhanced SIC in acidic soils but decreased SIC in alkaline soils
- SIC responses to afforestation also showed high variabilities among different species of tree plantations and across soil depths

Supporting Information:

Supporting Information may be found in the online version of this article.

Correspondence to:

A. Chen,
anping.chen@colostate.edu

Citation:

Hong, S., & Chen, A. (2022). Contrasting responses of soil inorganic carbon to afforestation in acidic versus alkaline soils. *Global Biogeochemical Cycles*, *36*, e2021GB007038. https://doi.org/10.1029/2021GB007038

Received 14 APR 2021
Accepted 21 DEC 2021

Abstract Afforestation is recommended as an effective approach for carbon sequestration and environmental benefits. However, it remains less clear, and sometimes controversial, regarding how afforestation may impact soil inorganic carbon (SIC), a crucial component of the ecosystem carbon pool. Using field data from 619 afforested plots and 163 control plots across northern China, we here investigated the relative and absolute differences in SIC between afforested and corresponding control plots. Our results suggested that afforestation increased SIC in acidic soils, while decreased SIC in alkaline soils. Fitting a linear mixed model and further a structure equation model, we found that afforestation-induced soil pH change was the most significant factor regulating SIC responses. In particular, SIC was more sensitive to pH change in more arid areas, where both soil pH and SIC stocks were high. Other factors could indirectly affect SIC responses to afforestation through modulating soil pH and soil organic carbon (SOC) dynamics. Moreover, afforestation-induced SIC changes also varied considerably among different species of tree plantations and across different soil depths. Importantly, in plantations of *Pinus sylvestris* var. *mongholica*, *Pinus tabuliformis*, and *Populus* spp., changes in SIC caused by afforestation were even comparable to that in SOC. Overall, our findings provide a data-based understanding on the comprehensive soil carbon dynamics following afforestation and its underlying mechanisms. With the increased use of afforestation and reforestation as nature-based solutions to climate change, their associated impacts on SIC need to be taken into account, especially in SIC-rich areas.

1. Introduction

Globally about 950 petagrams (Pg) carbon is stored in soils in inorganic form (Schlesinger, 1990; Schlesinger & Andrews, 2000). The size of this global soil inorganic carbon (SIC) pool is smaller than that of soil organic carbon (SOC, 1,550 Pg, Lal, 2004) but more than that of vegetation carbon (450–650 Pg, Friedlingstein et al., 2020). This large SIC pool is usually considered stable and thus has received little attention, especially when compared with SOC (Zamanian et al., 2018). However, SIC can regulate global C cycle both directly through absorbing and releasing CO_2 (Emmerich, 2003) and indirectly through affecting soil physical and chemical properties (Bowman et al., 2008). Moreover, several recent local-scale studies showed considerable SIC responses to agricultural management and land use changes (e.g., fertilization, afforestation, and grassland restoration), therefore challenging the conventional notion treating SIC as an inert carbon component (An et al., 2019; Bughio et al., 2016; Han et al., 2018; Kim et al., 2020). In particular, SIC is sensitive to soil acidification caused by nitrogen deposition and fertilization, and to land use changes and shrub encroachment (An et al., 2019; S. Liu et al., 2020; Yang, Fang, et al., 2012). Because SIC provides important soil buffering especially in alkaline soils (Bowman et al., 2008), its changes could modify soil buffering capacity and soil pH (Bowman et al., 2008; Hong et al., 2019; Yang, Fang, et al., 2012), and thus impact soil health and vegetation productivities (Bughio et al., 2016, 2017; Chang et al., 2012; S. Liu et al., 2020; Skyllberg, 1996; Yang, Ji, et al., 2012). Yet, to date, research on SIC dynamics is still very scarce and mostly localized. With extensive and long-term land use changes being a key feature characterizing global environmental changes (IPCC, 2021; Piao et al., 2018), improved understanding of their impacts on SIC over a broad geographical range is desired but largely missing in the literature.

Over recent decades, afforestation has been extensively adopted in many countries and regions for economic, ecological and climate change mitigation purposes (Bastin et al., 2019; Bonan, 2008). Afforestation can reduce soil erosion (H. Fang & Sun, 2017; Porto et al., 2009), regulate local and regional climate (Cerasoli et al., 2021; Peng et al., 2014; Y. Li et al., 2020) and enhance carbon sequestration (J. Fang & Chen, 2001; Peichl et al., 2012). From a carbon cycle perspective, the increase of vegetation biomass and SOC by afforestation has been reported

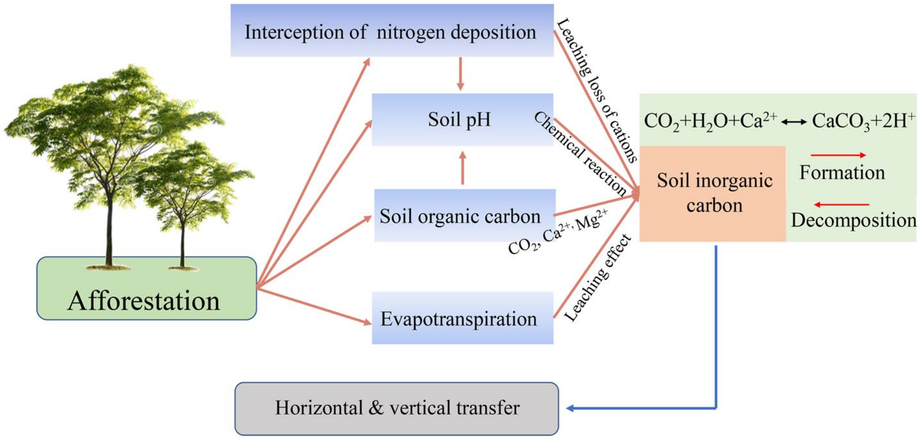

Figure 1. A concept diagram on how afforestation affects soil inorganic carbon.

by many studies (e.g., Cheng et al., 2016; A. Chen et al., 2019; Duffy et al., 2020; J. Fang & Chen, 2001; Laganière et al., 2010). However, it remains poorly understood how afforestation may influence SIC (Jia et al., 2019).

Since the dynamic of SIC is mainly determined by the formation and decomposition of carbonate, possible impacts of afforestation on SIC can in principle be understood through examining pathways in regulating soil carbonate dynamics, as depicted in Figure 1. First, afforestation could modify soil pH (Berthrong et al., 2009; Hong et al., 2018; Rhoades & Binkley, 1996), a key variable that is significantly correlated with carbonate stocks (Bowman et al., 2008; Hong et al., 2019). For instance, on soils with relatively higher pH, afforestation tends to acidify soils (Hong et al., 2018, 2019), which in return could dissolve carbonate and lead to SIC loss. Second, for places where afforestation enhances SOC, the increase of SOC could stimulate soil microbial respiration and release more porous CO_2 gases and Ca^{2+} and Mg^{2+} ions, which are known to help the formulation of carbonates (An et al., 2019). Third, afforestation changes land surface roughness and hence its interception of nitrogen deposition (Högberg et al., 2006). The increase of nitrate nitrogen (mainly NO_3^-) may enhance the leaching loss of base cations (e.g., Ca^{2+} and Mg^{2+}) on the charge balance of soil solutions (Gundersen et al., 2011; Lu et al., 2018); while that of ammonium nitrogen (mainly NH_4^+) can directly replace the base cations (Matschonat & Matzner, 1996). Both processes could lead to the decrease of base cations and thus the decomposition of SIC. Fourth, afforestation affects evapotranspiration and thus could change the amount and depth of water infiltrating into the soil (Basche & Delonge, 2019; Yao et al., 2016), through which SIC may be lost to deeper layers or down-streams (Slessarev et al., 2016). While all these processes have the potential to differentially influence how SIC may respond to afforestation, however, the overall impact of afforestation on SIC is still poorly understood and quantified.

Based on data collected with a paired control-afforestation sampling method in northern China, we previously showed that afforestation tended to increase soil pH in acidic soils but decrease soil pH in alkaline soils (Hong et al., 2018). Considering the strong relationship between soil pH and carbonate dynamics (Hong et al., 2019; Slessarev et al., 2016), we hypothesized that afforestation would increase/decrease SIC in acidic/alkaline soils. Our earlier study also demonstrated differentiated effects of afforestation on SOC (Hong et al., 2020). Accordingly, we also hypothesized that this afforestation-induced SOC change played a secondary role in regulating SIC responses to afforestation. Finally, given the large effects of afforestation on soil pH and SOC as revealed in our previous studies, we conjectured that changes in SIC following afforestation would be substantial. To test these hypotheses, we measured SIC contents for the same soil samples collected from 163 control plots and 619 afforested plots across northern China (Figure 2, see Section 2 for details). We used a linear mixed model (LMM) and a structure equation model (SEM) to disentangle the influences of various environmental factors on the SIC responses to afforestation.

10.1029/2021GB007038

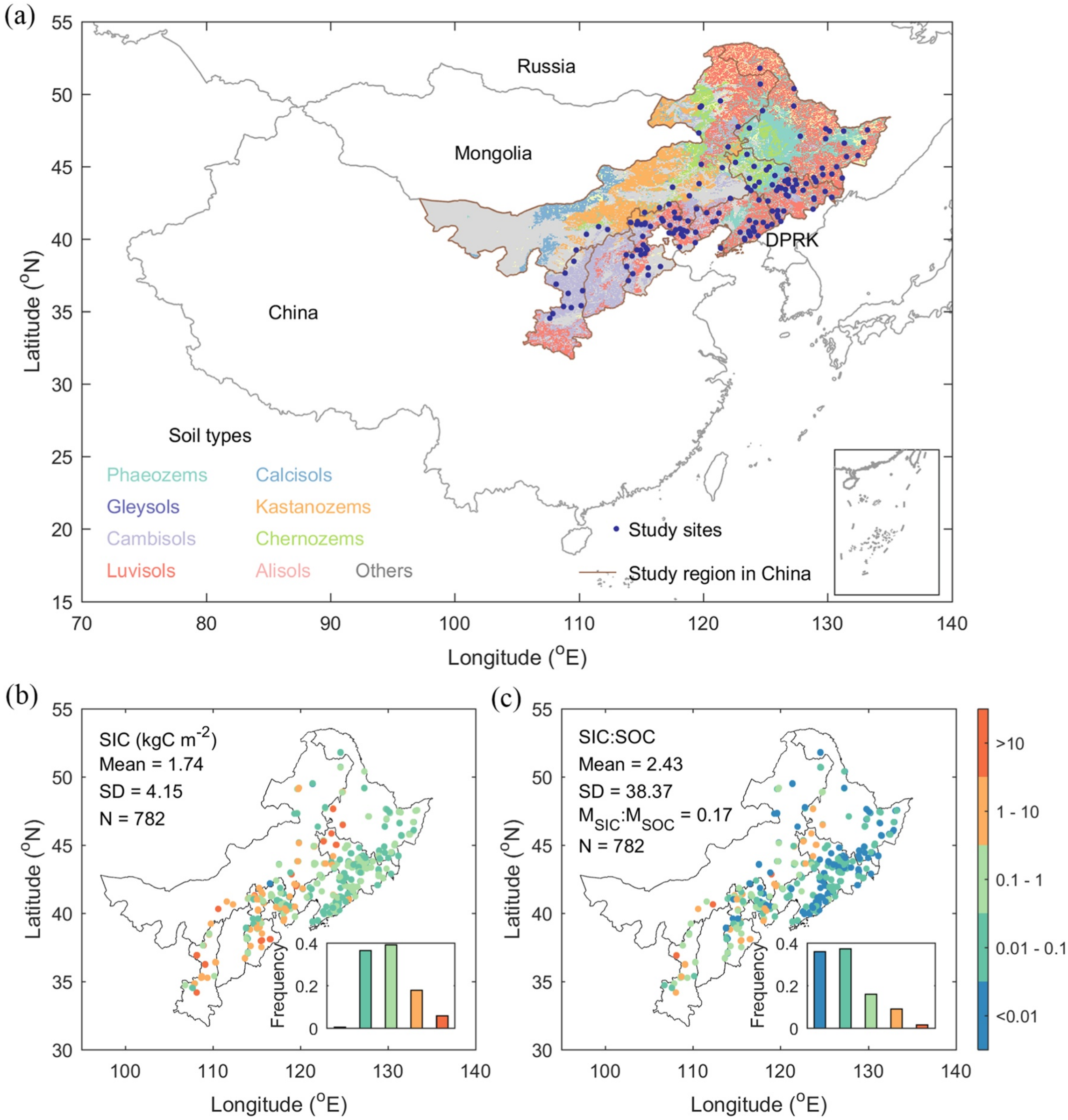

Figure 2. The study area and the spatial and statistical distributions of soil inorganic carbon (SIC) contents. (a) Soil types in the study area and the locations of field sites. Each site contains one control plot and usually multiple afforestation plots. (b) The spatial distribution of SIC. (c) The spatial distribution of the ratio between SIC and soil organic carbon (SOC). Data from both control and afforestation plots are shown in panels (b and c). Insets in panels (b and c) show the frequency distributions of the data. Panels (b and c) and their insets use the same color bar. M_{SIC}: M_{SOC} in panel (c) is the ratio between average SIC and average SOC across all the plots.

2. Materials and Methods

2.1. Study Region

Soil samples were collected from northern China covering the provinces of Heilongjiang, Jilin, Liaoning, Hebei, Shanxi, Shaanxi, and the Inner Mongolia (34.20°–51.80°N and 106.81°–133.31°E; Figure 2), where major afforestation and ecological restoration projects have been widely implemented over the past few decades. This region contains more than 120,000 km^2 of forest plantations, including the well-known Three-North Shelterbelt Development Program (FAO, 2016; Piao et al., 2009). Climate in this large area is highly diverse, with mean annual temperature (MAT) ranging from −3°C to 15°C and mean annual precipitation (MAP) from 355 to 1068 mm. Dominant soil types in this region include phaeozems, gleysols, humic cambisols, haplic/albic luvisols or eutric/dystric cambisols, haplic calcisols, kastanozems, chernozems, cambisols, haplic alisols, and

10.1029/2021GB007038

ferric/haplic luvisols, following the United Nations Food and Agriculture Organization (FAO) soil classification system (FAO et al., 2012; Xiong & Li, 1987). This region has also been reported with intense atmospheric nitrogen deposition (more than 20 kg N ha^{-1} per year) over the last few decades, with significant impacts on soil properties and plant productivities (X. Liu et al., 2013; Zhao et al., 2017). Overall, northern China offers an ideal place to investigate how afforestation may impact SIC dynamics across broad geographical and environmental ranges given its large-scale afforestation projects, diverse climate and soil properties, and intense nitrogen deposition.

2.2. Sampling Design

Soil samples were collected from 163 sites, each comprised one control plot and 1–26 afforested plots, across the study area (Figure 2a). That is, for most sites, one control plot could correspond to multiple afforested plots with different planted tree species and/or stand ages, while each afforested plot corresponded to one and only one control plot (Figure S1 in Supporting Information S1). In total, we obtained data from 163 control plots and 619 afforested plots, each of which was 20 × 20 m. These 163 control plots and 619 afforested plots constituted 619 control-afforestation pairs. The distance between any afforested plot and its corresponding control plot was usually 50–100 m (up to 2.5 km in very rare cases due to field or logistic constraints, see Figure S1 in Supporting Information S1) to minimize their differences in soil and climatic properties. Based on historical land use records provided by local forestry administrations, we also ensured that each control-afforestation pair shared the same pre-afforestation vegetation and soil types. Hence, the only difference between each paired control and afforested plots was afforestation versus no-afforestation, while they shared the same topography, climate, soil type and pre-afforestation vegetation type. This sampling design has also been successfully used in many previous studies (e.g., Friggens et al., 2020; Hong et al., 2020; Rowe et al., 2016).

Pre-afforestation vegetation and land use types in this study included cropland, barren land, grassland, natural forest, and riparian sand land. All the afforested plots were monocultured, with common tree species including *Pinus koraiensis*, *Larix gmelinii*, *Pinus sylvestris* var. *mongholica*, *Pinus tabuliformis*, and *Populus* spp. (including *Pop. simonii*, *Pop. beijingensis*, and *Populus* × *xiaohei*), and some other species such as *Robinia pseudoacacia* L. and *Diospyros kaki* Thunb. (collectively grouped as "others"). Together these five major tree species account for >70% of the planted area in the study area (Table S1 in Supporting Information S1). Information of each plot's stand age was obtained from records of local forestry administrations.

For each plot, we sampled soils from three replicate soil profiles on the diagonal direction, each at six different depths (0–5, 5–10, 10–20, 20–30, 30–60, and 60–100 cm; with a few exceptions when soil depths were less than 1 m), using a cutting ring of 100 cm^3. For each depth, we collected two identical cutting rings of soils, one of which would later be over-dried while the other air-dried.

2.3. Laboratory Method

All soil samples were brought back to the laboratory and dried. We weighed oven-dried soils and calculated each sample's bulk density based on the sample's dry weight and the volume of the cutting ring. Roots and stones were removed from air-dried samples, which then passed through 2-mm sieves and were prepared for chemical analyses. The pH of each sample was measured in 1:2.5 mixtures of soil and deionized water with a pH meter (PHS-3C, Lei-ci, China). Soil inorganic C content (SICC) was measured with a 08.53 CALCIMETER (M1.08.53.E, Eijkelkamp, Netherlands). Here, SICC was equivalent to the carbonate value measured by carbon dioxide (CO_2) emission of HCl (0.2 mol L^{-1}) acid-digested samples. Note for comparison, we also calculated soil organic carbon content (SOCC), which was the difference between total soil C content (STCC; measured with an Viro el cube, Elementar, Germany) and SICC.

2.4. Environmental Data Sets

The following environmental data sets were used to explore potential environmental controls of SIC responses to afforestation. MAP and MAT were obtained from the China Meteorological Forcing Data set, which has a spatial resolution of 0.1° × 0.1° and a temporal resolution of three hours (Y. Chen et al., 2011; Yang et al., 2010). Data of potential evapotranspiration (PET) were acquired from the Climate Research Unit (CRU) TS3.21 database with a 0.5° × 0.5° spatial resolution (Harris et al., 2014). We used PET rather than actual evapotranspiration

10.1029/2021GB007038

because PET is independent of precipitation and therefore could carry more information of climatic aridity (Lian et al., 2021; Slessarev et al., 2016). Water balance (WB) was estimated as the difference between MAP and PET (WB = MAP-PET). Data of atmospheric nitrogen deposition were obtained from the Multi-Scale Synthesis and Terrestrial Model Intercomparison Project (https://doi.org/10.3334/ORNLDAAC/1220) for the period of 2003–2012. This data set includes ammonium nitrogen (NHx) and nitrate nitrogen (NOx) depositions at a resolution of 0.5° × 0.5° (Wei et al., 2014). Data of soil type and clay content were obtained from the Harmonized World Soil Database v.1.2 (FAO, 2012). All the plot-level environmental data were extracted from the above-mentioned datasets based on the longitude and latitude of each plot.

2.5. Data Analysis

For each soil layer j, we calculated its SIC (SIC_j, kgC m^{-2}) using $SICC_j$ (%), bulk density (BD_j, g cm^{-3}), and the thickness of the layer (w_j, cm):

$$\mathrm{SIC}_j = \mathrm{SICC}_j \times \mathrm{BD}_j \times w_j \times 10^{-1} \tag{1}$$

Since each plot included three replicate profiles, we used mean SIC_j of the three profiles in data analysis. The sum of mean SIC_j for all the layers is thus SIC of each plot:

$$\mathrm{SIC} = \sum_{j=1}^{6} \mathrm{SIC}_j \tag{2}$$

We defined ΔSIC induced by afforestation as the difference between SIC in the afforested plots (SIC_f) and that in the control plots (SIC_c) at both the plot and layer levels (Equation 3). As afforestation may also change soil bulk density (Lee et al., 2009), we used soil mass of the control group as the equivalent mass and corrected the result of afforested group based on this equivalent mass.

$$\Delta\mathrm{SIC} = \mathrm{SIC\_f} - \mathrm{SIC\_c} \tag{3}$$

We also defined the response ratio (RR) of SIC as:

$$\mathrm{RR\_SIC} = \log_{10}\left(\frac{\mathrm{SIC\_f}}{\mathrm{SIC\_c}}\right) \tag{4}$$

Here, ΔSIC is the absolute change of SIC while RR_SIC is the relative change.

We also performed similar estimations for SOC changes and responses to afforestation (Hong et al., 2020):

$$\Delta\mathrm{SOC} = \mathrm{SOC\_f} - \mathrm{SOC\_c} \tag{5}$$

$$\mathrm{RR\_SOC} = \log_{10}\left(\frac{\mathrm{SOC\_f}}{\mathrm{SOC\_c}}\right) \tag{6}$$

Because pH value is the negative logarithm of hydrogen ion concentration, to estimate the mean pH of each soil profile and each plot from its multiple samples, we need to first convert pH values to hydrogen ion concentrations, $[H^+]$ (Hong et al., 2018). The mean concentration of hydrogen ions (H_p) for the entire soil profile was calculated from hydrogen ion concentration of each layer weighted by its mass ($w_j \times BD_j$):

$$H_p = \frac{\sum_{j=1}^{6} H_j \times w_j \times \mathrm{BD}_j}{\sum_{j=1}^{6} w_j \times \mathrm{BD}_j} \tag{7}$$

where H_j is the concentration of hydrogen ions of the jth layer. Similarly, the mean concentration of hydrogen ions over a plot was calculated by averaging H_p of its three replicate profiles. We then got the average pH for each plot from by log-transforming the average H_p.

The change in soil pH (ΔpH) was calculated as the difference between the averaged soil pH in afforested (pH_f) and control plots (pH_c):

$$\Delta\mathrm{pH} = \mathrm{pH\_f} - \mathrm{pH\_c} \tag{8}$$

We conducted the following statistical analyses to explore the effects of afforestation on SIC. A Wilcoxon rank sum test was used to compare SIC values in afforested and control groups since the data did not strictly satisfy the assumption of a normal distribution. Ordinary least squared regressions were performed to identify the relationships between variables. Furthermore, a LMM was employed to compare RR_SIC among different control-afforestation plot pairs and test how RR_SIC could be affected by environmental factors. The LMM method has been widely used in ecological and geographical studies (Laganière et al., 2010; Rowe et al., 2016) and was appropriate here considering mixed natures of different types of influence variables. The LMM in this study included 13 fixed explanatory variables (tree species, original vegetation and land use type (OVLUT), ΔpH, ΔSOC, pH in control group (pH_c), SOC in control group (SOC_c), SIC in control group (SIC_c), MAT, WB, NOx, NHx, stand age, and clay content), and one random variable (the control plot number, i.e., the site number) accounting for potential site effects since some afforested plots shared the same control plot. The interaction between tree species and OVLUT was also evaluated with the model.

We also fitted a piecewise SEM to explore potential pathways (and mechanisms) through which afforestation may affect SIC. Predictor variables in the SEM included ΔpH, ΔSOC, pH_c, SOC_c, SIC_c, MAT, WB, NOx, NHx, stand age, and clay content. We again added the control plot number into the model as a random variable. We fitted the component models of the piecewise SEM as linear models. The standardized coefficient of each path from each component model was reported. The overall fit of the SEM was evaluated using Shipley's test of d-separation: Fisher'C statistic and the Akaike Information Criterion. We used the R package "nlme" in R version 4.1.1 (R Core Team, 2021) to conduct LMM and "piecewiseSEM" to conduct piecewise SEM. All the other statistical analysis was conducted using MATLAB R2016b (MathWorks, Natick, MA, USA).

3. Results

3.1. Changes of SIC With Afforestation

Over the entire study area, the average SIC density (0–1 m depth) was 1.74 kgC m^{-2}, with a very large variation (SD = 4.15 kgC m^{-2}; Figure 2b). For comparison, the average SOC density (0–1 m depth) was 10.14 kgC m^{-2} (SD = 7.49 kgC m^{-2}). For most (76%) of the plots, SIC density was found in the range of 0.01–1 kgC m^{-2} (Figure 2b inset). SIC density was higher in more arid areas, such as the west of the study area. Across the entire area, SIC was about 17% of SOC. However, the SIC: SOC ratio was also highly variable and skewed toward the low end, with most (73%) of the ratio values falling in the range of 0–0.1 (Figure 2c inset) but an unusually high mean value of 2.43 (Figure 2c, SD = 38.37). This high mean value of the SIC: SOC ratio was due to extremely higher SIC than SOC at some locations.

Across the 619 control-afforestation pairs, the average of RR_SIC was −0.03 (Figure 3, SD = 0.74, $p = 0.41$), indicating an overall non-significant change in SIC with afforestation. Specifically, afforestation decreased SIC in 329 pairs from an average value of 2.07 to 0.83 kgC m^{-2}; while increased SIC in the remaining 290 pairs from 1.19 to 2.69 kgC m^{-2} on average. The overall change of SIC in the 0–1 m depth was 0.05 kgC m^{-2} (SD = 3.23 kgC m^{-2}, $p = 0.41$) (Figure 3).

The response of SIC to afforestation varied across tree species and depths (Figure 3). In general, afforestation significantly decreased SIC at depths of 0–5 and 60–100 cm, while had non-significant impacts at other depths. Species-wise, afforestation caused significant SIC decreases at top soils (0–5 cm) with *P. sylvestris* var. *mongholica*, and *P. tabuliformis*, and at 60–100 cm with *L. gmelinii*. Afforestation with *P. koraiensis*, *Populus* spp. and others resulted in divergent, although non-significant, changes in SIC at different depths.

3.2. Factors Controlling the Dynamics of SIC After Afforestation

The LMM analysis showed that SIC_c, ΔpH, ΔSOC, and stand age could explain most of the spatial variability in RR_SIC, while the effects of other factors, such as climate (WB and MAT), planted tree species, OVLUT, were insignificant (Table 1).

We further fitted a piecewise SEM to quantify the direct and indirect effects of these above factors on afforestation-caused SIC changes (Figure 4). Categorical variables including tree species and OVLUT were not included in the SEM considering the non-significant effects of these factors and their interactions according to the LMM results. We found ΔpH (change in soil pH resulted from afforestation) was the most significant variable ($\beta = 0.43$,

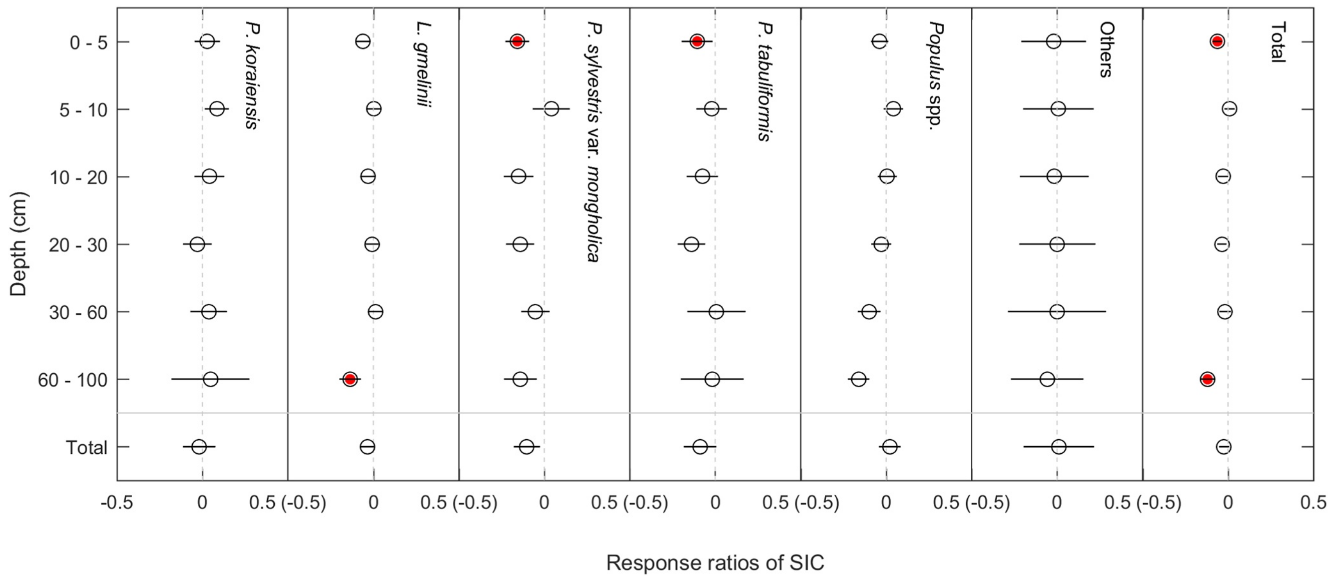

Figure 3. The response ratio of soil inorganic carbon to afforestation with different tree species at different depths. Cycles are the median values while error bars indicate the standard errors. Red points indicate $p < 0.05$ with the Wilcoxon rank sum test, meaning significant differences between the control and afforestation groups.

standardized coefficient, $p < 0.001$) determining RR_SIC. Changes in SOC (ΔSOC) also showed a significant effect ($\beta = 0.09$, $p < 0.05$) on RR_SIC. Hence, afforestation seems to impact SIC primarily through modifying soil pH and SOC. Background SIC ($\beta = -0.30$, $p < 0.001$), stand age ($\beta = -0.06$, $p < 0.05$), and MAT ($\beta = 0.16$, $p < 0.05$) also showed significant impacts on afforestation-induced SIC changes. Meanwhile, direct effects of

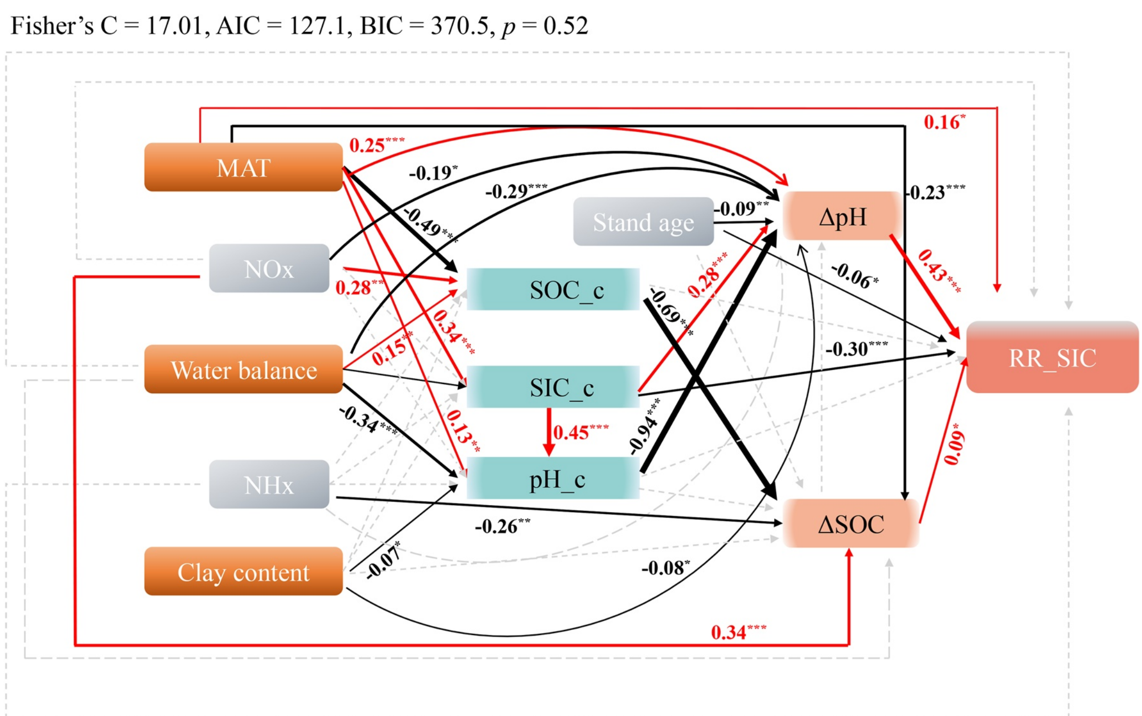

Figure 4. A structure equation model for the response ratio of soil inorganic carbon (RR_SIC). Solid red and black arrows represent significantly ($p < 0.05$) positive and negative paths, respectively; and gray dashed lines indicate non-significant pathways. Numbers near these lines are corresponding standard path coefficients. Arrow width is proportional to the strength of a relationship. Control plot number was added into the model as a random variable. A summary for all the variables is shown in Table S2 in Supporting Information S1.

Table 1
Results of a Linear Mixed Model for the Response Ratio of SIC

Factor	df	*F*	*p*
Species	5	2.06	ns
OVLUT	4	2.18	ns
Stand age	**1**	**4.72**	*
Water balance	1	0.03	ns
MAT	1	2.13	ns
SOC_c	1	2.21	ns
SIC_c	**1**	**11.61**	***
pH_c	1	1.76	ns
ΔSOC	**1**	**6.83**	**
ΔpH	**1**	**78.16**	***
NHx	1	0.45	ns
NOx	1	0.99	ns
Clay content	1	1.18	ns
Species × OVLUT	13	1.51	ns

Note. Control plot number was added into the model as a random variable. *$p < 0.05$; **$p < 0.01$; ***$p < 0.001$; ns, non-significant. Significant factors are highlighted in bold. The factor "Species × OVLUT" signifies the interaction of tree species and original vegetation and land use type. SOC_c, SIC_c, and pH_c are soil organic carbon (SOC), soil inorganic carbon (SIC), and soil pH in the control group, respectively; while ΔSOC, ΔSIC, and ΔpH indicate afforestation-induced changes in SOC, SIC, and soil pH, respectively. NHx and NOx indicate the deposition of ammonium and nitrate nitrogen, respectively; and MAT is the mean annual temperature.

other variables, including WB, nitrogen deposition, clay content, background SOC and soil pH, were weak and non-significant. However, these variables could still affect SIC dynamics indirectly through modulating soil pH and SOC. It is noteworthy that the strongest effect in the SEM was between ΔpH and pH_c, indicating that background soil pH strongly determined post-afforestation soil pH dynamics ($\beta = -0.94$, $p < 0.001$).

Based on the SEM results, we picked ΔpH, the most important determining factor for RR_SIC variations, and analyzed its correlations with RR_SIC and ΔSIC. We found a strong positive correlation between ΔpH and RR_SIC (Figure 5a, $p < 0.001$). Negative RR_SIC values were usually observed in alkaline (high pH) soils, where afforestation generally decreased soil pH. In contrast, positive values of RR_SIC were generally observed in acidic (low pH) soils, where afforestation tended to increase soil pH. This positive correlation between SIC responses and ΔpH was also confirmed when replacing RR_SIC with ΔSIC in the analysis (Figure 5b). In addition, the sensitivity of ΔSIC to ΔpH variations, that is, the regression slope between ΔSIC and ΔpH, increased with background soil pH, indicating that SIC in alkaline soils was more sensitive to changes in soil pH than that in acidic soils.

Interestingly, larger changes in SIC density was more often found in arid areas where SIC stocks were also usually higher (Figure S2 in Supporting Information S1). In areas with SIC density higher than 1 kgC m^{-2}, ΔSIC was negatively correlated with WB (MAP-PET). The largest loss of SIC was observed in areas with a water deficiency (negative WB) of about 200 mm yr^{-1}.

The determining role of soil pH on post-afforestation SIC changes was observed for all the tree species (Figure 6). Negative RR_SIC was usually observed when soil pH was higher than 7, and *L. gmelinii* showed the most significant negative response. When soil pH was lower than 7, positive RR_SIC was commonly observed, and the "others" afforestation group showed the most significant positive response (Figure 6a). For ΔSIC, afforestation with

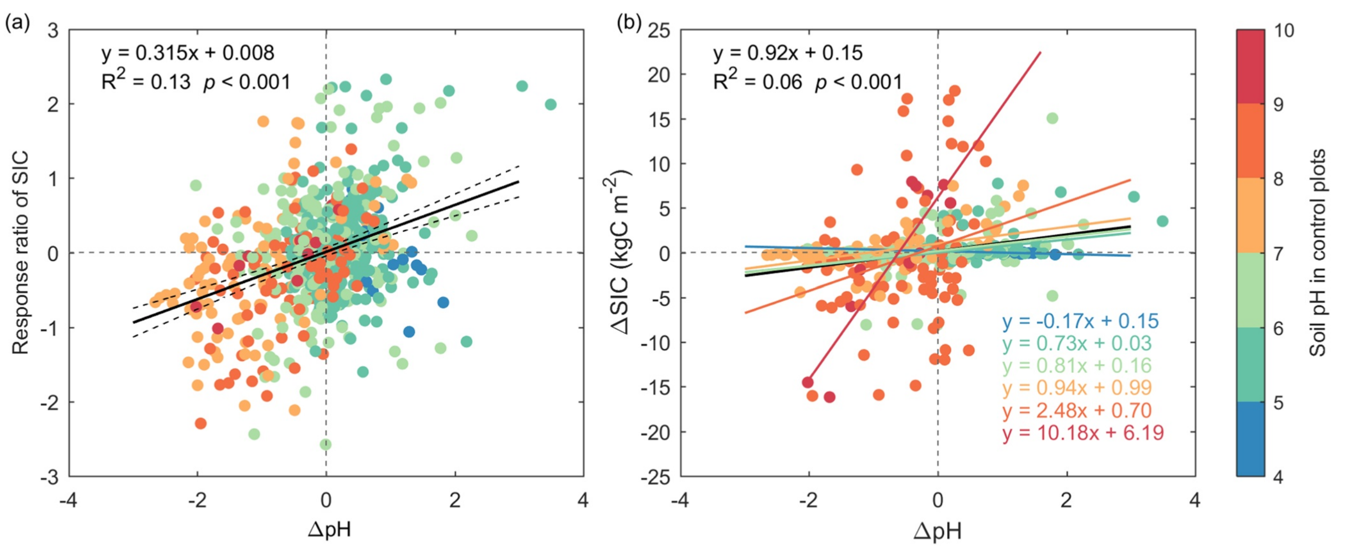

Figure 5. The relationships between ΔpH (pH in afforestation groups–pH in control groups) and (a) the response ratio of soil inorganic carbon (RR_SIC) and (b) ΔSIC (SIC in afforested groups–SIC in control groups). The two panels share the same color bar. The solid line in panel (a) is the result of an ordinary least squares (OLS) regression with all the data, and dashed lines mark the 95% confidence interval of the regression. In panel (b), the black line is the result of OLS regression with all the data, while lines in other colors represent the regression results for each soil pH group.

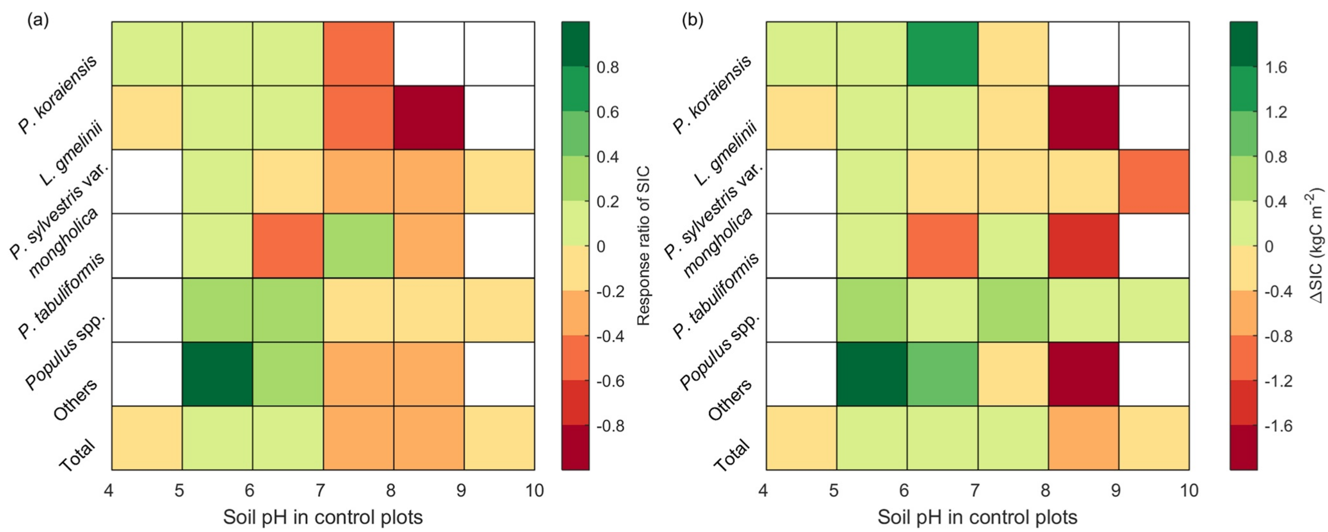

Figure 6. The effects of afforestation on soil inorganic carbon (SIC) across different tree species in soils with different pH ranges. Panel (a) shows the response ratios of SIC (RR_SIC), while panel (b) shows the absolute change of SIC (ΔSIC).

L. gmelinii, *P. tabuliformis*, and the "others" group resulted in the largest carbon loss in soils with pH > 8; while *P. koraiensis* and the group of "others" had the largest carbon gain in soils with pH < 7 (Figure 6b).

3.3. Contribution of SIC to Post-Afforestation Soil Carbon Dynamics

Across the whole region, the averaged change in SIC was 0.05 kgC m^{-2} (SD = 3.23 kgC m^{-2}, $p = 0.41$). This insignificant ΔSIC was smaller than the mean value of ΔSOC across the same sites (0.30 kgC m^{-2}). Both SOC and SIC showed divergent responses to afforestation, but we found no significant linkages between their dynamics (Figure S3 in Supporting Information S1). As summarized in Figure 7, ΔSOC and ΔSIC were both positive in 159 out of the 619 control-afforestation pairs. In this group, mean values of ΔSOC and ΔSIC were 6.57 and 1.46 kgC m^{-2}, respectively. By contrast, they were both negative in 167 pairs, with mean values of −6.22 and −0.97 kgC m^{-2}, respectively. Changes in SOC and SIC showed opposite directions for the remaining 293 pairs (131 for negative ΔSOC and positive ΔSIC, and 162 for positive ΔSOC and negative ΔSIC).

The change in SIC contributed differentially to soil carbon dynamics across different tree species (Figure 7). For *P. koraiensis* and *L. gmelinii* afforested plots, the contribution from afforestation-induced SIC changes to the overall soil carbon variation was negligible. However, for afforested forests of *P. sylvestris* var. *mongholica*, afforestation-induced changes in SIC made a substantial contribution to the total soil carbon dynamics at sites with positive ΔSOC. Changes in SIC and SOC even showed similar contributions to the total soil carbon dynamics for the afforestation groups of *P. tabuliformis*, *Populus* spp., and others (Figure 7).

4. Discussion

With field data collected from more than 700 plots over a broad geographical range in northern China, we provided a comprehensive evaluation on the effects of afforestation on SIC, an often-overlooked quantity in the research of carbon cycle dynamics. In general, we found that afforestation showed divergent effects on SIC, dependent on soil pH, afforestation tree species, and soil depths. However, for those species and soil depths where afforestation showed a significant impact on SIC, the impact was always negative (Figure 3). This negative impact was mostly observed at surface soil layers. Therefore, our finding suggested that SIC, especially surface SIC, is still sensitive to possible soil biophysical and biogeochemical changes caused by afforestation.

In explaining the relative change in SIC with afforestation, we found that RR_SIC is well correlated with ΔpH, indicating the sensitivity of SIC to changes in soil pH (S. Liu et al., 2020). Given that pH value is the negative logarithm of hydrogen ion concentration, this correlation between RR_SIC and ΔpH indicates that the dynamics of SIC and hydrogen ions are synergetic, confirming our earlier finding based on a spatial analysis (Hong

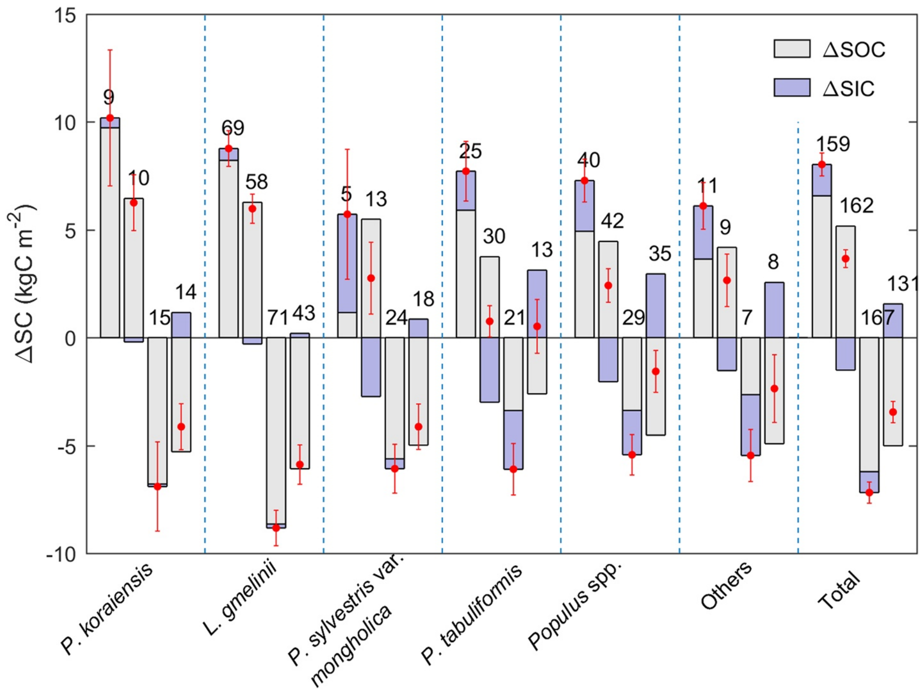

Figure 7. Changes in soil inorganic carbon (ΔSIC) and soil organic carbon (ΔSOC) resulted from afforestation with different tree species. For each tree species, four categories were identified based on combinations of change directions in SIC and SOC (i.e., positive ΔSOC and positive ΔSIC, positive ΔSOC and negative ΔSIC, negative ΔSOC and negative ΔSIC, and negative ΔSOC and positive ΔSIC). Red points indicate the change of total soil carbon (ΔSC = ΔSIC + ΔSOC) and error bars are the standard errors. The numbers near the bar mark the sample size of each group.

et al., 2019). Soil pH and SIC are closely linked at local and regional scales, and SIC provides a major buffering capacity to soil pH especially in arid areas (Bowman et al., 2008; Hong et al., 2019). At the local scale, changes in soil pH could also impact the decomposition and formation of SIC. Previously, we found that afforestation would reduce soil pH in alkaline soils while increase soil pH in acidic soils (Hong et al., 2018). Mechanisms responsible for afforestation-induced soil pH neutralization include changes in litter decomposition and rhizospheric processes, and modulations of ion cycles in soils (Ca^{2+}, Mg^{2+}, K^{+}, Al^{3+}, etc.) (Hong et al., 2018). This tendency of soil pH neutralization by afforestation could be the main cause underlying the divergent SIC responses to afforestation observed in this study. Specifically, in acidic soils, afforestation-induced soil pH increase could enhance the formation of carbonate. In contrast, afforestation-induced soil acidification in alkaline soils could partly dissolve SIC, which is usually in the form of carbonate (Raza et al., 2020). These mechanisms also explain the finding of the large carbon loss in SIC-rich soils during 1980s–2000s by an early study (Yang, Fang, et al., 2012).

Afforestation-induced changes in SOC provides another pathway modifying the response of SIC to afforestation. The accumulation of SOC would increase CO_2 and base cations like Ca^{2+} and Mg^{2+} (due to the increase of substrates and priming effect) in soil solutions, which could prevent the dissolution of SIC and enhance the formation of SIC (An et al., 2019). Furthermore, organic acids produced by the decomposition of SOC may also affect soil pH and thus SIC (Hong et al., 2018), although this effect might be weak and non-significant. Many studies on afforestation-, or more generally, land use change-induced, soil carbon dynamics, focus on either SIC or SOC. As we revealed here, the dynamics of SIC and SOC could be linked, weak in some groups or regions but strong in other groups or regions. Our current research on SIC responses to afforestation, together with our earlier work on the afforestation effects on SOC over the same region (Hong et al., 2020), provides a unique opportunity to understand the effects of afforestation on both SIC and SOC and their potential linkages in temperate northern China. Nonetheless, more comprehensive studies focusing on dynamics of both SOC and SIC over many different regions are needed to explore soil C cycles after land use changes.

Other environmental variables, such as nitrogen deposition and WB, seem to have weak or non-significant effects on RR_SIC. This little role of nitrogen deposition on RR_SIC seems to be in contrast with our earlier finding

10.1029/2021GB007038

that nitrogen deposition is a critical factor regulating the spatial patterns of SIC and pH (Hong et al., 2019). We suspect that this controversy could be caused by the little difference in nitrogen deposition between adjacent control and afforested plots, which may not be captured by the 0.5° × 0.5° gridded nitrogen deposition data set (Wei et al., 2014). Moreover, afforestation can increase the capture of N deposition due to increased surface roughness (Högberg et al., 2006), or decrease the amount of N reaching soils due to canopy interception (Wang et al., 2021), which would result in complex effects on soil pH and SIC. As the hydrological effects of afforestation could also affect carbonate leaching in soils and lead to vertical redistribution of SIC (S. Liu et al., 2020), SIC loss is generally observed in arid areas, where the leaching effect is weak (Chang et al., 2012) and may result in limited vertical reallocation (S. Liu et al., 2020). Surprisingly, we also observed non-significant effects of OVLUT on SIC responses to afforestation. As our samples spanned a broad geographical range even for the same OVLUT, there was a large variation in soil pH within each OVLUT group (Figure S4 in Supporting Information S1). The strong relationship between RR_SIC and ΔpH, as was observed in all the OVLUT groups (Figure S4 in Supporting Information S1), could overshade potential local-scale (where soil pH could be assumed invariant) effects of OVLUT on RR_SIC.

Our study provided a field data-based analysis of SIC changes with afforestation across a broad range of climates from arid to humid areas. While several previous studies have also investigated SIC dynamics with afforestation or land use changes, they were generally confined to arid areas with high soil pH and large SIC stocks (An et al., 2019; Yang, Ji, et al., 2012). Our results indicated that the relative change in SIC by afforestation was closely related to soil pH dynamics across a water deficit gradient, with the absolute change in SIC more sensitive to afforestation-induced pH change in soils with higher pH and SIC stocks. This higher sensitivity of SIC to afforestation in alkaline soils may be due to the greater availability of substrates for soil pH neutralization reactions. Considering the significant acidification resulted from afforestation in alkaline soils (Hong et al., 2018), these results indicate a high vulnerability of SIC in arid areas. Therefore, areas with high SIC stocks should be carefully evaluated for afforestation to minimize potential soil carbon loss.

The loss of SIC by afforestation could be detrimental to soil health and ecosystem productivity (Bowman et al., 2008; Skyllberg, 1996). In arid ecosystems, SIC plays an even more important role in carbon storage (Han et al., 2018). SIC in the form of carbonate also provides a major buffering capacity to soil pH changes in these regions (Bowman et al., 2008). The decrease of SIC by afforestation may imply a reduction in soil buffering capacity. Considering the high risk of soil acidification caused by increasing nitrogen and sulfur deposition in these regions, this reduction in soil buffering capacity may lead to positive feedbacks between soil acidification and carbonate loss (Ito et al., 2018; Yang, Ji, et al., 2012). Carbonate dissolution also drives the losses of base cations such as Ca^{2+}, Mg^{2+}, and K^+, and could further decrease soil fertility (S. Liu et al., 2020). A global meta-analysis suggested that afforestation resulted in a significant loss of base cations, especially for pine plantations (Berthrong et al., 2009). Given the essential role of exchangeable base cations for plant physiological processes, their losses would limit long-term ecosystem productivities (Binkley et al., 1989). Moreover, SIC loss would decrease the binding of organic matters on Ca^{2+}, and thus decrease its stability (Rowley et al., 2017). Therefore, the dynamic of SIC plays an important role in global carbon cycle and ecosystem health through direct and indirect pathways, and afforestation-caused SIC losses should be avoided or at least reduced as much as possible.

Large-scale afforestation is regarded as an effective anthropogenic interference to increase ecosystem carbon storage and mitigate climate change. The augmentation of planted forests worldwide is known to regulate local climate, reduce soil erosion, increase carbon storage in plant biomass and potentially also SOC (D. Li et al., 2017; Y. Li et al., 2018). Our findings, however, suggest that afforestation significantly impacts SIC storage, primarily through affecting soil pH. This finding challenges the conventional belief that SIC stocks are generally stable and play a minor role in global carbon cycle. For some afforestation tree species, such as *P. sylvestris* var. *mongholica*, *P. tabuliformis*, and *Populus* spp., changes in SIC are even comparable to that in SOC, suggesting that the estimation of carbon dynamics under afforestation or other land use changes should not neglect SIC responses. The total carbon sequestration by afforestation (including biomass, SOC and SIC) are highly variable, determined by climates, soil properties, tree species choices, and human management. Considering these high variabilities, the estimation that afforestation has the potential to offset 68% of global CO_2 emissions by an earlier study (Bastin et al., 2019) may be overly optimistic. Our findings also underscore the importance of carefully evaluating the climate and soil conditions and choosing appropriate planted tree species for maximizing the benefits while minimizing potential detriments by afforestation.

5. Conclusions

In this study, we comprehensively assessed how afforestation may impact SIC storage across diverse climate and ecosystem types with extensive field data from northern China, a hotspot of large-scale afforestation projects. Our results demonstrated a primary role of soil pH on controlling post-afforestation SIC dynamics. Specifically, post-afforestation SIC increased over acidic soils but decreased over alkaline soils. In addition to soil pH, factors such as SOC, species of tree plantations, and soil depths may also modulate SIC responses to afforestation. For some species, afforestation-induced SIC changes were even comparable to that in SOC, challenging the notion of stable SIC stocks that play a minor role in carbon cycle. We also showed that SIC was more sensitive to afforestation in SIC-rich arid areas, where future afforestation decisions need to be more carefully designed and implemented to achieve intended ecological and climate benefits.

Data Availability Statement

The field data related to this research are available at figshare (https://doi.org/10.6084/m9.figshare.16680613).

Acknowledgments
This study was supported by the National Key R&D Program of China (2019YFA0607304) and the Strategic Priority Research Program (A) of the Chinese Academy of Sciences (grant XDA20050101). A.C. is partly supported by a DOE grant (DE-SC0022074), and S.H. acknowledges the support from the Postdoctoral Innovation Talents Support Program of China (Grant No. BX2021005). The authors thank many formal members of Dr. Shilong Piao's group at the Peking University, including Guodong Yin, Nan Cong, and Jie Liu, for assistance in the field and laboratory work. Dr. Hui Zeng of Peking University Shenzhen Graduate School generously provided resources and lab space for carbon measurements. The authors are also grateful to Dr. Jonay Jovani and another, anonymous, reviewer for their helpful comments and suggestions on early versions of this manuscript.

References

An, H., Wu, X., Zhang, Y., & Tang, Z. (2019). Effects of land-use change on soil inorganic carbon: A meta-analysis. *Geoderma*, *353*, 273–282. https://doi.org/10.1016/j.geoderma.2019.07.008

Basche, A., & Delonge, M. (2019). Comparing infiltration rates in soils managed with conventional and alternative farming methods: A meta-analysis. *PLoS One*, *14*(9), e0215702. https://doi.org/10.1371/journal.pone.0215702

Bastin, J. F., Finegold, Y., Garcia, C., Mollicone, D., Rezende, M., Routh, D., et al. (2019). The global tree restoration potential. *Science*, *365*, 76–79. https://doi.org/10.1126/science.aax0848

Berthrong, S. T., Jobbágy, E. G., & Jackson, R. B. (2009). A global meta-analysis of soil exchangeable cations, pH, carbon, and nitrogen with afforestation. *Ecological Applications*, *19*, 2228–2241. https://doi.org/10.1890/08-1730.1

Binkley, D., Valentine, D., Wells, C., & Valentine, U. (1989). An empirical analysis of the factors contributing to 20-year decrease in soil pH in an old-field plantation of loblolly pine. *Biogeochemistry*, *8*, 39–54. https://doi.org/10.1007/bf02180166

Bonan, G. B. (2008). Forests and climate change: Forcings, feedbacks, and the Climate benefits of forests. *Science*, *320*, 1444–1449. https://doi.org/10.1126/science.1155121

Bowman, W. D., Cleveland, C. C., Halada, L., Hresko, J., & Baron, J. S. (2008). Negative impact of nitrogen deposition on soil buffering capacity. *Nature Geoscience*, *1*, 767–770. https://doi.org/10.1038/ngeo339

Bughio, M. A., Wang, P., Meng, F., Chen, Q., Li, J., & Shaikh, T. A. (2017). Neoformation of pedogenic carbonate and conservation of lithogenic carbonate by farming practices and their contribution to carbon sequestration in soil. *Journal of Plant Nutrition and Soil Science*, *180*, 454–463. https://doi.org/10.1002/jpln.201500650

Bughio, M. A., Wang, P., Meng, F., Qing, C., Kuzyakov, Y., Wang, X., & Junejo, S. A. (2016). Neoformation of pedogenic carbonates by irrigation and fertilization and their contribution to carbon sequestration in soil. *Geoderma*, *262*, 12–19. https://doi.org/10.1016/j.geoderma.2015.08.003

Cerasoli, S., Yin, J., & Porporato, A. (2021). Cloud cooling effects of afforestation and reforestation at midlatitudes. *Proceedings of the National Academy of Sciences*, *118*(33), e2026241118. https://doi.org/10.1073/pnas.2026241118

Chang, R., Fu, B., Liu, G., Wang, S., & Yao, X. (2012). The effects of afforestation on soil organic and inorganic carbon: A case study of the Loess Plateau of China. *Catena*, *95*, 145–152. https://doi.org/10.1016/j.catena.2012.02.012

Chen, A., Peng, S., & Fei, S. (2019). Mapping global forest biomass and its changes over the first decade of the 21st century. *Science China Earth Sciences*, *62*, 585–594. https://doi.org/10.1007/s11430-018-9277-6

Chen, Y., Yang, K., He, J., Qin, J., Shi, J., Du, J., & He, Q. (2011). Improving land surface temperature modeling for dry land of China. *Journal of Geophysical Research*, *116*, D20104. https://doi.org/10.1029/2011jd015921

Cheng, J., Lee, X., Tang, Y., Pan, W., Gao, W., Chen, Y., et al. (2016). Changes in above- and below-ground nitrogen stocks and allocations following the conversion of farmland to forest in rocky desertification regions. *Agriculture, Ecosystems & Environment*, *232*, 9–16. https://doi.org/10.1016/j.agee.2016.07.019

Duffy, C., O'Donoghue, C., Ryan, M., Styles, D., & Spillane, C. (2020). Afforestation: Replacing livestock emissions with carbon sequestration. *Journal of Environmental Management*, *264*(1), 110523. https://doi.org/10.1016/j.jenvman.2020.110523

Emmerich, W. (2003). Carbon dioxide fluxes in a semiarid environment with high carbonate soils. *Agricultural and Forest Meteorology*, *116*, 91–102. https://doi.org/10.1016/s0168-1923(02)00231-9

Fang, H., & Sun, L. (2017). Modelling soil erosion and its response to the soil conservation measures in the black soil catchment, Northeastern China. *Soil and Tillage Research*, *165*, 23–33. https://doi.org/10.1016/j.still.2016.07.015

Fang, J., & Chen, A. (2001). Dynamic forest biomass carbon pools in China and their significance. *Acta Botanica Sinica*, *43*(9), 967–973.

FAO. (2016). *Global Forest Resources Assessment 2015*. Food and Agricultural Organization of the United Nations.

FAO, IASA, ISRIC, ISSCAS, & JRC. (2012). *Harmonized world soil database (version 1.2)*. FAO and IIASA.

Friedlingstein, P., O'Sullivan, M., Jones, M., Andrew, R., Hauck, J., Olsen, A., et al. (2020). Global carbon budget 2020. *Earth System Science Data*, *12*, 3269–3340. http://doi.org/10.5194/essd-12-3269-2020

Friggens, N., Hester, A., Mitchell, R., Parker, T., Subke, J., & Wookey, P. A. (2020). Tree planting in organic soils does not result in net carbon sequestration on decadal timescales. *Global Change Biology*, *26*(9), 5178–5188. https://doi.org/10.1111/gcb.15229

Gundersen, P., Schmidt, I., & Raulund-Rasmussen, K. (2011). Leaching of nitrate from temperate forests – Effects of air pollution and forest management. *Environmental Reviews*, *14*(1), 1–57. https://doi.org/10.1139/a05-015

Han, X., Gao, G., Chang, R., Li, Z., Ma, Y., Wang, S., et al. (2018). Changes in soil organic and inorganic carbon stocks in deep profiles following cropland abandonment along a precipitation gradient across the Loess Plateau of China. *Agriculture, Ecosystems & Environment*, *258*, 1–13. https://doi.org/10.1016/j.agee.2018.02.006

Harris, I., Jones, P. D., Osborn, T. J., & Lister, D. H. (2014). Updated high-resolution grids of monthly climatic observations—the CRU TS3.10 Dataset. *International Journal of Climatology*, *34*(3), 623–642. https://doi.org/10.1002/joc.3711

Högberg, P., Fan, H., Quist, M., Binkley, D. A. N., & Tamm, C. O. (2006). Tree growth and soil acidification in response to 30 years of experimental nitrogen loading on boreal forest. *Global Change Biology*, *12*, 489–499. https://doi.org/10.1111/j.1365-2486.2006.01102.x

Hong, S., Gan, P., & Chen, A. (2019). Environmental controls on soil pH in planted forest and its response to nitrogen deposition. *Environmental Research*, *172*, 159–165. https://doi.org/10.1016/j.envres.2019.02.020

Hong, S., Piao, S., Chen, A., Liu, Y., Liu, L., Peng, S., et al. (2018). Afforestation neutralizes soil pH. *Nature Communications*, *9*, 520. https://doi.org/10.1038/s41467-018-02970-1

Hong, S., Yin, G., Piao, S., Dybzinski, R., Cong, N., Li, X., et al. (2020). Divergent responses of soil organic carbon to afforestation. *Nature Sustainability*, *3*, 694–700. https://doi.org/10.1038/s41893-020-0557-y

IPCC. (2021). In V. Masson-Delmotte, P. Zhai, A. Pirani, S. L. Connors, C. Péan, S. Berger, et al. (Eds.), *Climate Change 2021: The Physical Science Basis. Contribution of Working Group I to the Sixth Assessment Report of the Intergovernmental Panel on Climate Change*. Cambridge University Press.

Ito, A., Nishina, K., Ishijima, K., Hashimoto, S., & Inatomi, M. (2018). Emissions of nitrous oxide (N_2O) from soil surfaces and their historical changes in East Asia: A model-based assessment. *Progress in Earth and Planetary Science*, *5*, 55. https://doi.org/10.1186/s40645-018-0215-4

Jia, X., Wang, X., Hou, L., Wei, X., Zhang, Y., Shao, M., & Zhao, X. (2019). Variable response of inorganic carbon and consistent increase of organic carbon as a consequence of afforestation in areas with semiarid soils. *Land Degradation & Development*, *30*, 1345–1356. https://doi.org/10.1002/ldr.3320

Kim, J., Jobbágy, E., Richter, D., Trumbore, S., & Jackson, R. (2020). Agricultural acceleration of soil carbonate weathering. *Global Change Biology*, *26*, 5988–6002. https://doi.org/10.1111/gcb.15207

Laganière, J., Angers, D., & Paré, D. (2010). Carbon accumulation in agricultural soils after afforestation: A meta-analysis. *Global Change Biology*, *16*(1), 439–453. http://doi.org/10.1111/j.1365-2486.2009.01930.x

Lal, R. (2004). Soil carbon sequestration impacts on global climate change and food security. *Science*, *304*, 1623–1627. https://doi.org/10.1126/science.1097396

Lee, J., Hopmans, J., Rolston, D., Baer, S., & Six, J. (2009). Determining soil carbon stock changes: Simple bulk density corrections fail. *Agriculture, Ecosystems & Environment*, *134*(3), 251–256. https://doi.org/10.1016/j.agee.2009.07.006

Li, D., Wen, L., Zhang, W., Yang, L., Xiao, K., Chen, H., & Wang, K. (2017). Afforestation effects on soil organic carbon and nitrogen pools modulated by lithology. *Forest Ecology and Management*, *400*, 85–92. https://doi.org/10.1016/j.foreco.2017.05.050

Li, Y., Piao, S., Chen, A., Ciais, P., & Li, L. Z. X. (2020). Local and teleconnected temperature effects of afforestation and vegetation greening in China. *National Science Review*, *7*, 897–912. https://doi.org/10.1093/nsr/nwz132

Li, Y., Piao, S., Li, L. Z. X., Chen, A., Wang, X., Ciais, P., et al. (2018). Divergent hydrological response to large-scale afforestation and vegetation greening in China. *Science Advances*, *4*, eaar4182. https://doi.org/10.1126/sciadv.aar4182

Lian, X., Piao, S., Chen, A., Huntingford, C., Fu, B., Li, L. Z. X., et al. (2021). Multifaceted characteristics of dryland aridity changes in a warming world. *Nature Reviews Earth & Environment*, *2*, 232–250. https://doi.org/10.1038/s43017-021-00144-0

Liu, S., Zhou, L., Li, H., Zhao, X., Yang, Y., Zhu, Y., et al. (2020). Shrub encroachment decreases soil inorganic carbon stocks in Mongolian grasslands. *Journal of Ecology*, *108*, 678–686. https://doi.org/10.1111/1365-2745.13298

Liu, X., Zhang, Y., Han, W., Tang, A., Shen, J., Cui, fnm, et al. (2013). Enhanced nitrogen deposition over China. *Nature*, *494*, 459–462. https://doi.org/10.1038/nature11917

Lu, X., Vitousek, P., Mao, Q., Gilliam, F., Luo, Y., Zhou, G., et al. (2018). Plant acclimation to long-term high nitrogen deposition in an N-rich tropical forest. *Proceedings of the National Academy of Sciences*, *115*, 5187–5192. https://doi.org/10.1073/pnas.1720777115

Matschonat, G., & Matzner, E. (1996). Soil chemical properties affecting NH_4^+ sorption in forest soils. *Zeitschrift für Pflanzenernährung und Bodenkunde*, *159*, 505–511. https://doi.org/10.1002/jpln.1996.3581590514

Peichl, M., Leava, N., & Kiely, G. (2012). Above- and belowground ecosystem biomass, carbon and nitrogen allocation in recently afforested grassland and adjacent intensively managed grassland. *Plant and Soil*, *350*(1–2), 281–296. https://doi.org/10.1007/s11104-011-0905-9

Peng, S., Piao, S., Zeng, Z., Ciais, P., Zhou, L., Li, L. Z. X., et al. (2014). Afforestation in China cools local land surface temperature. *Proceedings of the National Academy of Sciences*, *111*, 2915–2919. https://doi.org/10.1073/pnas.1315126111

Piao, S., Fang, J., Ciais, P., Peylin, P., Huang, Y., Sitch, S., & Wang, T. (2009). The carbon balance of terrestrial ecosystems in China. *Nature*, *458*, 1009–1013. https://doi.org/10.1038/nature07944

Piao, S., Huang, M., Liu, Z., Wang, X., Ciais, P., Canadell, J., et al. (2018). Lower land-use emissions responsible for increased net land carbon sink during the slow warming period. *Nature Geoscience*, *11*, 739–743. https://doi.org/10.1038/s41561-018-0204-7

Porto, P., Walling, D., & Callegari, G. (2009). Investigating the effects of afforestation on soil erosion and sediment mobilisation in two small catchments in Southern Italy. *Catena*, *79*, 181–188. https://doi.org/10.1016/j.catena.2009.01.007

Raza, S., Na, M., Wang, P., Ju, X., Chen, Z., Zhou, J., & Kuzyakov, Y. (2020). Dramatic loss of inorganic carbon by nitrogen-induced soil acidification in Chinese croplands. *Global Change Biology*, *26*, 3738–3751. https://doi.org/10.1111/gcb.15101

R Core Team. (2021). R: A language and environment for statistical computing (Version 4.1.1). R Foundation for Statistical Computing. Retrieved from https://www.R-project.org/

Rhoades, C., & Binkley, D. (1996). Factors influencing decline in soil pH in Hawaiian Eucalyptus and Albizia plantations. *Forest Ecology and Management*, *80*, 47–56. https://doi.org/10.1016/0378-1127(95)03646-6

Rowe, R., Keith, A., Elias, D., Dondini, M., Smith, P., Oxley, J., & McNamara, N. P. (2016). Initial soil c and land-use history determine soil c sequestration under perennial bioenergy crops. *GCB Bioenergy*, *8*(6), 1046–1060. https://doi.org/10.1111/gcbb.12311

Rowley, M. C., Grand, S., & Verrecchia, E. (2017). Calcium-mediated stabilisation of soil organic carbon. *Biogeochemistry*, *137*, 27–49. https://doi.org/10.1007/s10533-017-0410-1

Schlesinger, W. H. (1990). Evidence from chronosequence studies for a low carbon-storage potential of soils. *Nature*, *348*, 232–234. https://doi.org/10.1038/348232a0

Schlesinger, W. H., & Andrews, J. A. (2000). Soil respiration and the global carbon cycle. *Biogeochemistry*, *48*, 7–20. https://doi.org/10.1023/a:1006247623877

Skyllberg, U. (1996). Small scale pH buffering in organic horizons of two boreal coniferous forest stands. *Plant and Soil*, *179*, 99–107. https://doi.org/10.1007/bf00011647

Slessarev, E., Lin, Y., Bingham, N., Johnson, J., Dai, Y., Schimel, J., & Chadwick, O. A. (2016). Water balance creates a threshold in soil pH at the global scale. *Nature*, *540*, 567–569. https://doi.org/10.1038/nature20139

Wang, X., Wang, B., Wang, C., Wang, Z., Li, J., Jia, Z., et al. (2021). Canopy processing of N deposition increases short-term leaf N uptake and photosynthesis, but not long-term N retention for aspen seedlings. *New Phytologist*, *229*, 2601–2610. https://doi.org/10.1111/nph.17041

Wei, Y., Liu, S., Huntzinger, D., Michalak, A., Viovy, N., Post, W., et al. (2014). *NACP MsTMIP: Global and North American driver data for multimodel intercomparison*. ORNL DAAC. https://doi.org/10.3334/ORNLDAAC/1220
Xiong, Y., & Li, Q. (1987). *Soils in China*. Press of Sciences.
Yang, K., He, J., Tang, W., Qin, J., & Cheng, C. C. K. (2010). On downward shortwave and longwave radiations over high altitude regions: Observation and modeling in the Tibetan Plateau. *Agricultural and Forest Meteorology*, *150*, 38–46. https://doi.org/10.1016/j.agrformet.2009.08.004
Yang, Y., Fang, J., Ji, C., Ma, W., Mohammat, A., Wang, S., et al. (2012). Widespread decreases in topsoil inorganic carbon stocks across China's grasslands during 1980s–2000s. *Global Change Biology*, *18*, 3672–3680. https://doi.org/10.1111/gcb.12025
Yang, Y., Ji, C., Ma, W., Wang, S., Wang, S., Han, W., et al. (2012). Significant soil acidification across northern China's grasslands during 1980s–2000s. *Global Change Biology*, *18*, 2292–2300. https://doi.org/10.1111/j.1365-2486.2012.02694.x
Yao, Y., Zeng, Z., Liu, Y., Peng, S., Zhu, Z., & Piao, S. (2016). The effect of afforestation on soil moisture content in Northeastern China. *PLoS One*, *11*, e016776. https://doi.org/10.1371/journal.pone.0160776
Zamanian, K., Zarebanadkouki, M., & Kuzyakov, Y. (2018). Nitrogen fertilization raises CO_2 efflux from inorganic carbon: A global assessment. *Global Change Biology*, *24*, 2810–2817. https://doi.org/10.1111/gcb.14148
Zhao, Y., Zhang, L., Chen, Y., Liu, X., Xu, W., Pan, Y., & Duan, L. (2017). Atmospheric nitrogen deposition to China: A model analysis on nitrogen budget and critical load exceedance. *Atmospheric Environment*, *153*, 32–40. https://doi.org/10.1016/j.atmosenv.2017.01.018